Absolute properties of the neglected eclipsing B-type binary HD 194495 [b]

Ömür Çakırlı [a], Esin Spahi [a] & Cafer İbanoğlu [a]

[a] *Ege University, Science Faculty, Astronomy and Space Sciences Dept., 35100 Bornova, İzmir, Turkey. e − mail: omur.cakirli@ege.edu.tr*

[b] *Based on observations collected at Catania Astrophysical Observatory (Italy)*

Abstract

We present the results of the high-resolution spectroscopic observations of the neglected binary system HD 194495 (B3 IV-V+B4 V). A combined analysis of three different photometric data set (*Tycho* B_T and V_T photometry, H_p-band data of *Hipparcos* and $V-$band data of ASAS3 photometry) and radial velocities indicates that the system has an orbital period of 4.90494 ± 0.00005 days and an inclination of 69±1 degrees. This solution yields masses and radii of $M_1 = 7.57\pm0.08$ $M_\odot$ and $R_1 = 5.82\pm0.03$ $R_\odot$ for the primary and $M_2 = 5.46\pm0.09$ $M_\odot$ and $R_2 = 3.14\pm0.08$ $R_\odot$ for the secondary. Based on the position of the two stars plotted on a theoretical H-R diagram, we find that the age of the system is $\gtrsim$ 28 Myr, according to stellar evolutionary models. The spectroscopic and photometric results are in agreement with those obtained using theoretical predictions.

Key words: Stars: binaries; Eclipsing stars: fundamental parameters; Individual Method: Spectroscopy; stars: HD 194495

1 Introduction

The masses and radii of stars are two fundamental parameters in stellar astrophysics. Accurate mass determinations of B–type stars still are urgently required, since actual masses are based on a very small number of eclipsing binaries. Data of this kind are important for tests of stellar models, with far-reaching implications such as modelling of stellar components of galaxies. Our main motivations to study this system to explain the nature of the B-star binary HD 194495. This effort is part of an ongoing research to determine the masses and radii of such systems.

The star HD 194495 was classified as B7 V single-lined, massive spectroscopic binary by Monet (1979). System consists of an evolved, more massive, and more luminous primary component and a main sequence secondary star. It has an eccentric orbit (e=0.14) and an orbital period of 4.90 days. Several radial velocity measurements of primary component of HD 194495 by Monet (1979) show range from -80 km s^{-1} to 100 km s^{-1}, but no further investigations were made into this probable velocity variable and radial velocity of the second component measurements. The eclipsing nature of its light curve was first noticed with the *Hipparcos* satellite (HIP 100719) and later *ASAS* photometric survey (ASAS 202511+2129.3) where it was classified as an *unsolved variables* eclipsing binary and known as V399 Vulpecula (Kazarovets et al., 1999).

As one of only a few eclipsing B-star binary HD 194495 provides a potentially important system because it is a test case for stellar structure and evolution models. It is critical that well-determined values for the current separation and component masses be determined. In this paper, we use the optical spectra of HD 194495 to reveal the nature of its light variability and physical properties in combination with the photometric data obtained by Hipparcos and ASAS-3 as well as with the our reconstruction of spectra. The paper is organized as follows. In §2 the spectroscopic observations, data analysis, temperature estimations, reddening and reconstruction of spectra are described. Derived absolute parameters of the stars from the combination spectroscopic and photometric results are given in §3. We compare the individual masses based on the spectroscopic and photometric orbits to those predicted by theoretical methods and discuss their implications in §4.

2 Spectroscopic observations

Spectroscopic observations have been performed with the échelle spectrograph (FRESCO) at the 91-cm telescope of Catania Astrophysical Observatory. The spectrograph is fed by the telescope through an optical fibre (UV–NIR, 100 μm core diameter) and is located, in a stable position, in the room below the dome level. Spectra were recorded on a CCD camera equipped with a thinned back–illuminated SITe CCD of 1k×1k pixels (size 24×24 μm). The cross-dispersed échelle configuration yields a resolving power R=$\lambda/\delta\lambda$=22 000, as deduced from the full width at half maximum of the lines of the Th–Ar calibration lamp. The spectra cover the wavelength range from 4300 to 6650 Å, split into 19 orders. In this spectral region, and in particular in the blue portion of the spectrum, there are several lines useful for the measure of radial velocity, as well as for spectral classification of the stars.

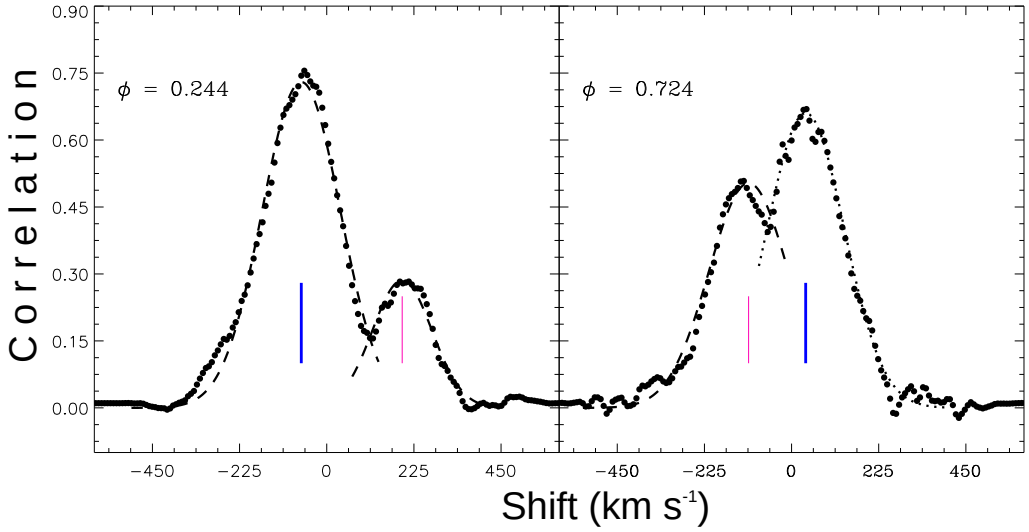

Fig. 1. Sample of Cross Correlation Functions between HD 194495 and the radial velocity template spectrum in first and second quadrature phase. The horizontal axis is relative radial velocities, and vertical axis is normalized cross-correlation amplitude. Note that splittings at stronger peaks. The phases of observations and the wavelength of the peak centers of the primary (thick bar) and secondary (thin bar) component are also marked.

The data reduction was performed by using the échelle task of IRAF [1] package following the standard steps: background subtraction, division by a flat field spectrum given by a halogen lamp, wavelength calibration using the emission lines of a Th-Ar lamp, and normalization to the continuum through a polynomial fit.

Seventeen spectra of HD 194495 were collected during the 20 observing nights between August 14 and September 22, 2007. Typical exposure times for the HD 194495 spectroscopic observations were between 2400 and 2600 s. The signal-to-noise ratio (S/N) achieved was between 70 and 120, depending on atmospheric condition. α Lyr (A0V), 59 Her (A3IV), ι Psc (F7V), HD 27962 (A2IV), and τ Her (B5IV) were observed during each run as radial velocity and/or rotational velocity templates. The average S/N at continuum in the spectral region of interest was 150–200 for the standard stars.

[1] IRAF is distributed by the National Optical Observatory, which is operated by the Association of the Universities for Research in Astronomy, inc. (AURA) under cooperative agreement with the National Science Foundation

Table 1
Radial velocities of the components of HD 194495. The columns give the heliocentric Julian date, the orbital phase, the radial velocities of the two components with the corresponding errors, and the average S/N of the spectrum.

HJD	Phase	Star 1		Star 2		$< S/N >$
2 454 300+		$\mathbf{V}_p$	σ	$\mathbf{V}_s$	σ	
27.4695	0.0500	-54	4.1	–	–	89
28.4235	0.2445	-144	1.2	160	4.6	120[a]
29.3672	0.4369	-35	5.0	–	–	97
30.4330	0.6542	80	1.6	-140	9.1	106
31.3786	0.8470	74	1.5	-137	9.9	95
33.4202	0.2632	-138	3.1	151	5.1	106[a]
35.3825	0.6633	78	1.2	-134	9.2	80
36.4028	0.8713	65	3.2	-127	8.1	90[a]
37.3967	0.0739	-73	4.2	–	–	90
38.3786	0.2741	-136	3.2	151	4.4	113[a]
43.3666	0.2910	-127	3.5	132	7.6	95
46.4666	0.9231	40	2.9	-87	11.1	97
48.3967	0.3165	-110	2.1	124	7.7	111[a]
50.3967	0.7243	90	3.0	-157	10.1	120[a]
64.4143	0.5822	56	1.5	-105	15.8	72
65.4489	0.7931	89	2.1	-152	4.1	115[a]
66.4121	0.9895	-6	6.2	–	–	90

[a] Used also for rotational velocities ($v \sin i$) measurements.

2.1 Spectroscopic analysis

The radial velocities of HD 194495 were obtained by cross–correlating of échelle orders of HD 194495 spectra with the spectra of the bright radial velocity standard stars α Lyr and τ Her (Nordström et al., 1963). For this purpose the IRAF task fxcor was used.

Figure 1 shows example of CCF at first and second quadrature phase. The two peaks correspond to each component of HD 194495. The stronger peaks in each CCF correspond to the more luminous component that have a larger weight into the observed spectrum. We adopted a two-Gaussian fit algorithm to re-

solve cross-correlation peaks near the second quadrature when spectral lines are visible separately. At this phase, absorption lines of the primary and secondary components of the system can be easily recognized in the range between 4300-6800 Å. These regions include the following lines: He I 4387 Å, Mg II 4481 Å, He I 4713, He I 5016 Å, He I 4917 Å, He I 5876 Å. We limited our analysis to the echelle orders in the spectral domains in the range, which include several photospheric absorption lines. We have disregarded very broad lines like H_α, H_β and H_γ because their broad wings affect the CCF and lead to large errors. A double-lined Gaussian fit was used to disentangle the CCF peaks and determine the RVs of each component. Following the method proposed by Penny et al. (2001) we first made two-Gaussian fits of the well separated CCFs using the deblending procedure in the IRAF routine splot. The average fitted FWHM is 234±8 and 178±9 km s^{-1} for the primary and secondary components, respectively. In Figure 1 we show a sample of double-Gaussian fit. Indeed, the shapes and velocities corresponding to the peaks of the CCFs are slightly changed. By measuring the areas enclosed by the Lorentzian profiles of the spectral lines belonging to the primary (A_1) and secondary (A_2) we estimate the light ratio of the primary star (F_1) to the secondary (F_2). In this way, we were able to obtain an estimate of the monochromatic flux ratio in the red and blue part of the spectra of $F_1/F_2 \sim A_1/A_2$=0.63 based upon the relative line depths of the spectral components.

2.1.1 Resulting radial velocities

The resulting radial velocities are listed in Table 1 together with their standard errors. The observational points and their error bars are displayed in Figure 2 as a function of orbital phase as calculated by means of the ephemeris (equation 1) and fixed it during the orbital solutions. Other parameters, such as the velocity semi-amplitude of the components ($K_{1,2}$), systemic velocity (V_γ), longitude of periastron (ω), orbital eccentricity (e), and time of periastron passage (T_0) were converged. The final solution gave K_1=116±4 km s^{-1}, K_2=161±6 km s^{-1}, Vγ=-15±1 km s^{-1}, ω=2.72±0.09, and e=0.12±0.07. Our spectroscopic mass ratio is q=M_2/M_1=0.72. Hence, our analysis gives the following parameters: $M_1 \sin^3 i$=6.16±0.05 $M_\odot$, $M_2 \sin^3 i$=4.44±0.06 $M_\odot$, and $a \sin i$=26.68±0.01 $R_\odot$.

2.2 Spectral classification and temperature estimates

We have used the spectra to reveal the spectral type of the primary component of HD 194495. For this purpose we have measured the equivalent widths (EW) of photospheric absorption lines for the spectral classification (Table 2). We have followed the procedures described by Hernández et al. (2004), choosing

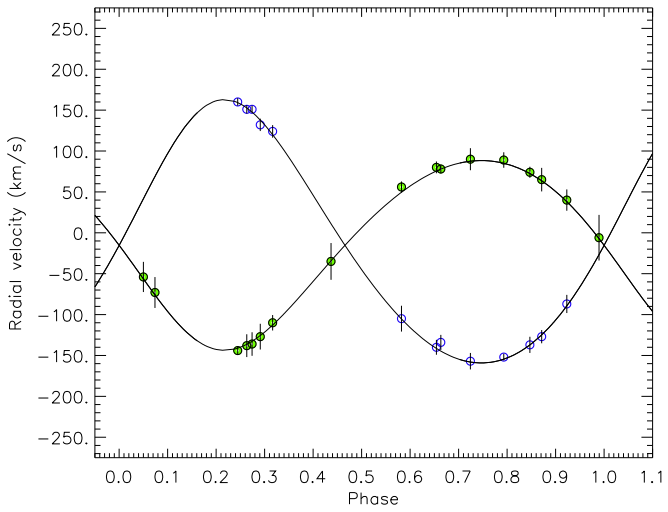

Fig. 2. Radial velocity curve folded on a period of 4.904938 days. Points with error bars (error bars are masked by the symbol size in some cases) show the radial velocity measurements for the components of the system (primary: filled circles, secondary: open circles).

Table 2
Equivalent widths of the selected lines in the spectra.

Spectral lines	$EW_{primary}$ (Å)
He I + Fe I λ 4922	0.26±0.11
Hγ λ 4349	0.37±0.11
He I λ 5876	0.35±0.13
He I+Fe I λ 4387	0.35±0.21
Hβ 4861	5.31±0.42

hydrogen and helium lines in the whole wavelength region, where the contribution of the primary component is considerably larger than that of the secondary in the spectra. From the calibration relations of EW–Spectral-type given by Hernández et al. (2004), we have derived a spectral type of B3±1 for the primary component. The effective temperature deduced from the calibrations of Drilling & Landolt (2000), and de Jager & Nieuwenhuijzen (1987) is 18 600±650 and 19 100±680 K for the primary component, respectively. The mean effective temperature of the primary component deduced from the spectra is therefore 19 000±550 K .

HD 194495 is listed in several large photometric databases consolidated in the *Hipparcos* Catalogue, which provide optical magnitudes of B=$7^m.09\pm0^m.02$, V=$7^m.07\pm0^m.01$. Since the magnitudes collected from photometric measure-

ments and the colors are inconsistent no attempt has been made to calculate the effective temperatures of the components. The infrared magnitudes are taken from 2MASS (Cutri et al., 2003) catalog as J=$7^m.159\pm0^m.009$, H=$7^m.221\pm0^m.017$, and K=$7^m.249\pm0^m.011$. The observed infrared colours of J-H=-$0^m.162\pm0^m.031$ and H-K=-$0^m.028\pm0^m.018$ correspond to a combined spectral type of B2±2 is an agreement with that we derived by spectral lines alone. Hence V-K, J-H and H-K colors of the primary component corresponds to a spectral type of B2±1.

2.3 Reddening

The measurement of reddening is a key step in determining the absolute temperature scale (and therefore the distance) of eclipsing binaries. In addition to moderate distance determined by the Hipparcos mission, some reddening is expected for HD 194495 due to its low galactic latitude (l=63°.03, $b = -9°.34$).

Our spectra cover the interstellar NaI (5890 and 5896 Å) doublets, which is excellent estimators of the reddening as demonstrated by Munari & Zwitter (1997). They calibrated a tight relation linking the Na I D2 (5890 Å) and KI (7699 Å) equivalent widths with the E(B-V) reddening. On spectra obtained at quadratures, lines from both components are un-blended with the interstellar ones, which can therefore be accurately measured. We derive an equivalent width of 0.21±0.03 Å for only NaI, which corresponds to E(B-V)= $0^m.08\pm0^m.02$. KI interstellar line is out of our spectral range as given in wavelength region in previous section.

2.4 Rotational velocity and reconstruction of spectra

The width of the cross-correlation profile is a good tool for the measurement of $v \sin i$ (see, e.g., Queloz et al. (1998)). The rotational velocities ($v \sin i$) of the two components were obtained by measuring the FWHM of the CCF peaks in ten high-S/N spectra of HD 194495 acquired close to the quadratures, where the spectral lines have the largest Doppler-shifts. In order to construct a calibration curve FWHM–$v \sin i$, we have used an average spectrum of HD 27962, acquired with the same instrumentation. Since the rotational velocity of HD 27962 is very low but not zero ($v \sin i \simeq$11 km s^{-1}, e.g., Royer et al. (2002)), it could be considered as a useful template rotating faster than $v \sin i \simeq$ 10 km s^{-1}. The spectrum of HD 27962 was synthetically broadened by convolution with rotational profiles of increasing $v \sin i$ in steps of 5 km s^{-1} and the cross-correlation with the original one was performed at each step. The FWHM of the CCF peak was measured and the FWHM-$v \sin i$ calibration was established. The $v \sin i$ values of the components of HD 194495 were derived

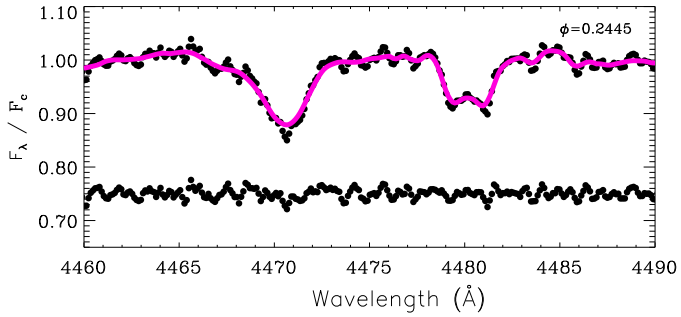

Fig. 3. Observed spectrum of HD 194495 (large dots) in the Mg II λ4481. The synthetic spectrum (B3V+B4V) is displayed with continuous line in the same boxes. The differences (observed-synthetic, shifted) are plotted in the bottom of panel.

from the FWHM of their CCF peak and the aforementioned calibration relations, for a few wavelength regions and for the best spectra. This gave values of 61±5 km s^{-1} for the primary star and 39±7 km s^{-1} for the secondary star.

We performed an accurate spectral classification and measured rotational velocities of the components in order to search for the best combination of the two standard-star spectra able to reproduce the observed spectrum of the HD 194495. From the observed two standard star spectra of, acquired with the same instrumentation, τ Her and α Lyr are used as standard stars for the primary and secondary, respectively. For the construction of the reproduced observed spectrum of the system the spectra of the τ Her (B5IV) and α Lyr (A0V) have been rotationally broadened by convolution with the appropriate rotational profile and then have co-added, properly weighted by using physical parameters (T_1, T_2, R_1, R_2, $v_{1,2}sini$) of the components as input parameters and Doppler-shifted according to the radial velocity solution derived in next section.

Figure 3 shows the reconstructed spectra for the primary and secondary with the best fit spectra overplotted. The relative depths of He I λ4471 and Mg II λ4481 are good temperature indicators throughout the B-star sequence (Williams , 2009) plus the H$_\gamma$ line that is sensitive to gravity (linear stark effect). Specifically, the He I λ4471 line gets weaker while the Mg II λ4481 line gets stronger as temperature decreases.

The resolving power of the instrument is unsuitable for attempting classical spectral typing. However, we can arrive at an estimate of the spectral types for each components in the HD 194495 system by comparing the derived effective temperatures in §2.2 and §3. According to the Table 2 of Böhm-Vitense (1981) the effective temperature and gravity of the primary of HD 194495 is most consistent with a B3 IV-V star while the secondary matches most closely with a B4 V star, and these classifications are listed in Table 3.

Table 3
Spectroscopic reconstruction parameters of the components.

Parameter	Primary	Secondary
Spectral Type	B3 IV-V[a]	B4 V[a]
T_{eff} (K)	19 000±320	18 250±520
log g (cgs)	3.79±0.25	4.18±0.25
$vsini$ (km s^{-1})	61±5	39±7
F_1/F_2	0.63±0.12	

[a] The spectral types are estimated from derived values of T_{eff} and log g.

3 Combined radial velocity and light curve solution

3.1 The binary ephemeris

Studying of the light curves was achieved on the basis of three different photometric data sets [Tycho B_T and V_T photometry, H_p-band data of Hipparcos and V-band data of ASAS3 (Pojmanski, 2002)]. Meaningfully photometric observations of HD 194495 were made by the Hipparcos mission and 78 H_p magnitudes were listed by van Leeuwen (2007). These magnitudes were obtained in a time interval of about three years. The accuracy of the Hipparcos data is about $\sigma_{H_p} \sim 0.01$. These measurements are plotted against the orbital phase in the bottom panel of Figure 4. In spite of their low precision, the Hipparcos and Tycho data clearly show light variation when the observations are phased with the ephemeris, limited by the lack of observations in the primary and secondary minima and by insufficient sensitivity.

The All Sky Automated Survey database contains light curves for ∼39 000 previously unknown variable stars. We extracted the V-band light curve for HD 194495 (*ASAS* 202511+2129.3) from this catalog, removing points deemed lower quality by the data reduction pipeline used by the ASAS. The 238 photometric measurements of ASAS, including eclipses, were used to determine the light-curve elements. All available photometric data are phased and rescaled in Figure 4. It is clear from Figure 4 that HD 194495 is an eccentric binary, with the secondary eclipse at phase 0.44 relative to the primary eclipse at phase 0.00. The scatter of the data in the out-of-eclipse phases was about $0^{\rm m}.03$.

The ASAS photometry permits determination of only one seasonal moment of primary eclipse, but this enable us to obtain an improved primary eclipse

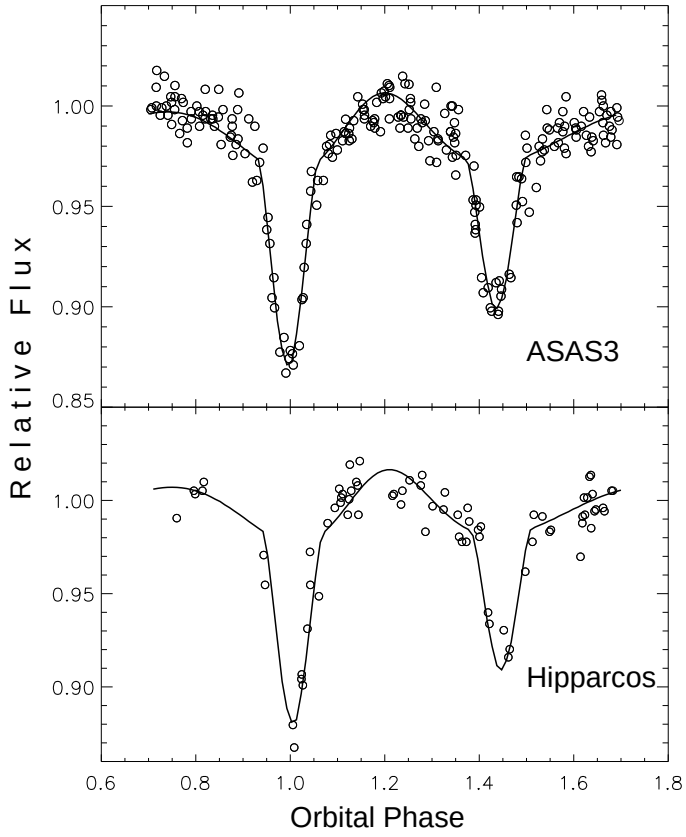

Fig. 4. The ASAS3-V band and H_p band light curves of HD 194495 with the best fit model overlaid as shown in Table 5.

ephemeris. We determine from the data an ephemeris of:

$$MinI(HJD) = 2\,452\,860.6478(25) + 4^d.904938(33) \times E \qquad (1)$$

where the errors in the last significant digits are given in parentheses.

3.2 Determination of the photometric elements

In order to reproduce the observed characteristics of the photometric light curves, we analysed them with the Wilson–Devinney code implemented into the PHOEBE package tool by Prša & Zwitter (2005) for the LC and differential correction (DC) fits. For the analysis, combined light curves of three data set was modelled. Considering the spectroscopic analysis the temperature of the primary was fixed to 19 000 K, and the bolometric albedo and gravity brightening coefficients were set to unity, as generally found for stars with the radiative envelopes (von Zeipel, 1924). The logarithmic limb darkening law

Table 4
Results from the simultaneous solution of $ASAS_V$ and $Hipparcos_{V_p}$ band light curves of HD 194495.

Parameter	ASAS+H_p
$i(^\circ)$	69±1
T_1 (K)	19 000[Fix]
T_2 (K)	17 900±70
Ω_1	5.690±0.038
Ω_2	7.054±0.057
q_{spec}	0.723[Fix]
$\frac{L_{1_{Hipp.}}}{(L_{1+2})_V}$	0.609±0.091
$\frac{L_{1_{ASAS3}}}{(L_{1+2})_V}$	0.630±0.091
r_1	0.2035±0.0013
r_2	0.1123±0.0017
χ^2	0.0211

was used and limb-darkening coefficients were taken from van Hamme (1993). The surface potential ($\Omega_{1,2}$), light factors of the components ($l_{1,2}$) and orbital inclination (i) were adjustable parameters during the light-curve modelling.

The mass ratio, q=M_2/M_1, is very important parameter in the light curve analysis, because the WD code is based on Roche geometry which is sensitive to this quantity. The mass ratio, eccentricity and longitude of periastron were determined from the radial velocity analysis was kept as a fix value. The iterations were carried out automatically until convergence and a solution was defined as the set of parameters for which the differential corrections were smaller than the probable errors. The combined light curve was analized and the weighted means of the parameters i, T_2, Ω_1, Ω_2, r_1 and r_2 were computed. Our final results are listed in Table 4 and the computed light curves are shown as continuous lines in Figure 4. The uncertainities assigned to the adjusted parameters are the internal errors provided directly by the Wilson-Devinney code.

Table 5
Fundamental parameters of HD 194495.

	HD 194495	
Parameter	Primary	Secondary
a ($R_\odot$)	28.58±1.12	
V_γ (km s^{-1})	-15±1	
q	0.723±0.003	
Mass ($M_\odot$)	7.57±0.08	5.46±0.03
Radius ($R_\odot$)	5.82±0.03	3.14±0.08
log g (cgs)	3.50±0.02	3.54±0.03
T_{eff} (K)	19 000±550	17 800±600
$(vsin\ i)_{obs}$ (km s^{-1})	61±2	39±4
$(vsin\ i)_{calc.}$ (km s^{-1})	60±1	32±1
log $(L/L_\odot)$	3.93±0.06	3.64±0.10
d (pc)	274±5	
J, H, K_s (mag)*	7.159±0.018, 7.221±0.027, 7.249±0.027	
$\mu_\alpha cos\delta$, μ_δ(mas yr^{-1})**	-0.48±0.59, -2.59±0.62	
U, V, W (km s^{-1})	36±1, -16±1, -18±2	

**2MASS* All-Sky Point Source Catalogue (Cutri et al., 2003)
***Newly Reduced Hipparcos Catalogue (van Leeuwen, 2007)

4 Discussion and conclusions

4.1 Absolute dimensions and distance to the system

Combination of the parameters obtained from light curves and RVs yield the absolute dimensions of the system, which are presented in Table 5. The standard deviations of the parameters have been determined by JKTABSDIM [2] code, which calculates distance and other physical parameters using several different sources for bolometric corrections (Southworth et al., 2005). The mass and radii of the components were estimated with uncertainities of 1 %.

An inspection of the temperatures, masses and radii of the component stars

[2] This can be obtained from http://www.astro.keele.ac.uk/∼jkt/codes.html

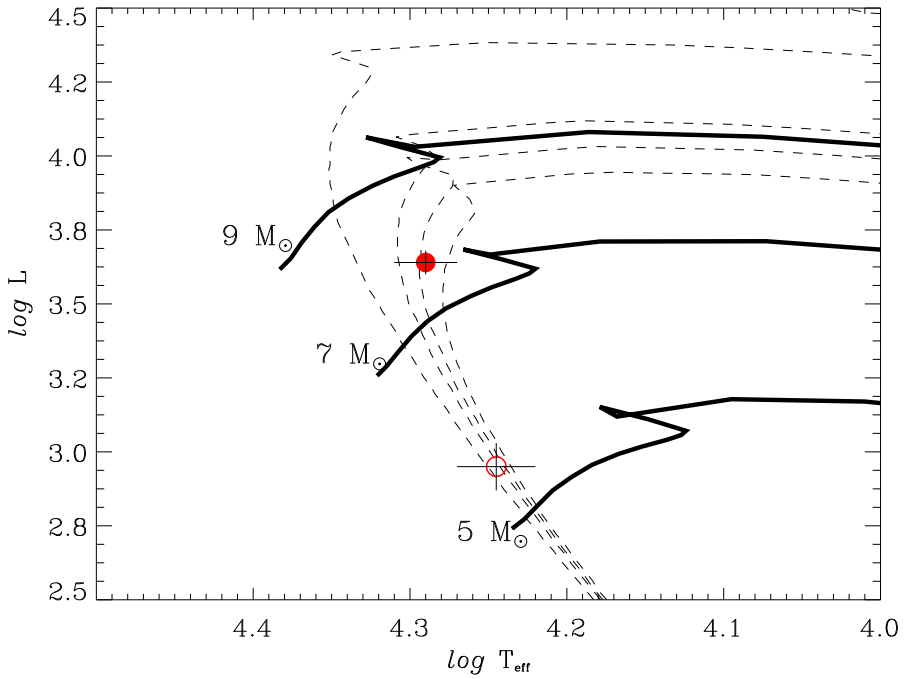

Fig. 5. Positions of the components of the system in HR diagram are plotted. The solid lines evolutionary tracks for stars of various masses from Schaller et al. (1992) and isochrones (vertical dashed lines) from Lejeune & Schaerer (2001) for solar metallicity with ages of 20, 25, 28, and 32 Myr going from left to right. The positions of the components are consistent with an age of $\sim$ 28 Myr.

reveals a binary system composed of two main-sequence stars. The temperature T_{eff1} = 19 000 K, mass M_1 = 7.58 $M_\odot$ and radius R_1 = 5.8 $R_\odot$ of the primary are consistent with the spectral type of B3, and the temperature T_{eff2} = 17 800 K, mass M_2 = 5.46 $M_\odot$ and radius R_2 = 3.1 $R_\odot$ of the secondary are consistent with an B4V spectral type star.

Using the two $E(B-V)$ values derived from photometric and spectroscopic data we calculated the de–reddening distance modulus of the system. To estimate the bolometric magnitudes of the components we adopted M_{bol}=4.74 mag for the Sun. Using the bolometric corrections given by Drilling & Landolt (2000) and Girardi et al. (2002) we estimate the distance to the system as 274 and 269 pc, respectively, with an uncertainity of 5 pc. However, the average distance to the system is estimated to be 290^{+42}_{-29} pc from the trigonometric parallax measured by the Hipparcos mission.

To compare the distance of HD 194495 using a different method we used a luminosity-colour relation (Bilir et al., 2008), which has been constructed for binary systems with main-sequence components. This method calculates the color excess ($E_d(B-V)$) in the direction and the distance of the HD 194495 using Schlegel et al. (1998) maps (see details in Bilir et al. (2008)). The re-

duced color excess in direction of the HD 194495 is calculated E_d(B-V)=0.072. The near-infrared magnitudes of the system were taken from the 2MASS Point Sources Catalogue of Cutri et al. (2003) and are shown in Table 5.

The colour excess $E(B-V) = 0.08$ was estimated in direction of HD 194495 by using equivalenth width of the interstellar lines. The near-infrared absolute magnitude of HD 194495 system was estimated by the luminosity-colour relation, $M_J = 5.228(J-H)_o + 6.185(H-K_s)_0 + 0.608$, of Bilir et al. (2008) and the distance of the system is calculated as 274±8 pc by using the photometric parallaxes method. The photometric distance of 274±8 pc given in Table 5 is consistent with the 269±8 pc and 290±8 pc distance estimated by studiying of the interstellar lines and the Hipparcos measurements, respectively.

4.2 Evolutionary stage and age of the system

We have presented the results of the masses and radii of the stars in the HD 194495 system to great accuracy and also a photometric solution of the system. The results of the light and radial velocity curves analysis of the allows to derive the absolute parameters of the system. We have determined the masses and radii of the two stars to 1% for the primary and secondary star. The resulting parameters of HD 194495 are given in Table 5. As is seen in Table 5, both stars of the system are well within their Roche radii but experience tidal distortion that is evident in the V-band light curve (Figure 4). The rotational velocities derived from the reconstructions (Table 3) very well match with the synchronous rotation values found from analysis. Therefore, this system has achieved synchronous rotation, and is not very young.

In order to discuss the evolutionary status of the components of the system, the locations of two stars were plotted on Hertzsprung – Russell (HR) diagram. In this HR diagram (Figure 5) plotted against evolutionary tracks for stars of 5, 7, and 9 $M_\odot$ from Schaller et al. (1992), as well as isochrones from Lejeune & Schaerer (2001) for solar metallicity with ages of 20, 25, 28, and 32 Myr. The location of the stars is most consistent with an age of $\sim$28 Myr. The positions of the components of the system appear in Figure 5 to be overluminous for the derived masses of $M_1 = 7.6$ $M_\odot$ for the primary and $M_1 = 5.5$ $M_\odot$ for the secondary. Table 15.7 of Tokunaga (1991) gives the astrophysical parameters for stars of the various spectral classes. The mass and effective temperature of the primary fit between the listed values for spectral types B3 (7.6 $M_\odot$) and B4 ($\sim$ 6.8 $M_\odot$), but the radius is much larger than the means for comparable spectral types and matches a B3 star (4.8 $R_\odot$). Hilditch et al. (2005) found several systems of comparable mass that, like HD 194495, are overluminous compared with model predictions for eclipsing binaries in the Small Magellanic Cloud (SMC) . However, the results for HD 194495 seem

to conflict with the results of Malkov (2003), who showed that early B-type stars that are in close systems and rotate more slowly than single stars are on average smaller than those same single stars. Malkov (2007) also studied well separated binaries in an effort to use the properties of their component stars for a more direct comparison with single stars. The mass–luminosity–radius relations in his study, when applied to our results for HD 194495, predict less-luminous, hotter, and smaller components. This is perhaps not surprising, due to the age of HD 194495 and the evolution of its components from the zero-age main sequence.

To study the kinematical properties of HD 194495, we used the system's center-of-mass' velocity, distance and proper motion values, which are given in Table 5. The proper motion data were taken from newly reduced Hipparcos catalogue (van Leeuwen, 2007), whereas the center-of-mass velocity and distance are obtained in this study. The system's space velocity was calculated using Johnson & Soderblom (1987) algorithm. The U, V and W space velocity components and their errors were obtained and given in Table 5. To obtain the space velocity precisely the first-order galactic differential rotation correction was taken into account (Mihalas & Binney, 1981), and -1.08 and 0.65 kms^{-1} differential corrections were applied to U and V space velocity components, respectively. The W velocity is not affected in this first-order approximation. As for the LSR correction, Mihalas & Binney (1981) values (9, 12, 7)$_{\odot}$ kms^{-1} were used and the final space velocity of HD 194495 was obtained as $S = 43$ kms^{-1}. This value is in agreement with other young stars space velocities given in the criterion from Leggett (1992) for young disc stars -50 $\leq$ U $\leq$ 20, -30 $\leq$ V $\leq$ 0, -25 $\leq$ W $\leq$ 10.

To determine the population type of HD 194495 the galactic orbit of the system was examined. Using Dinescu et al. (1999) N-body code, the system's apogalactic (R_{max}) and perigalactic (R_{min}) distances were obtained as 7.88 and 8.81 kpc, respectively. Also, the maximum possible vertical separation from the galactic plane is $|z_{max}|$=50 pc for the system. When determining the ellipticity the following formula was used:

$$e = \frac{R_{max} - R_{min}}{R_{max} + R_{min}}. \tag{2}$$

The ellipticity was calculated as $e = 0.06$. This value shows that HD 194495 is orbiting the Galaxy in an almost circular orbit and that the system belongs to the young thin-disc population.

Acknowledgment

We thank Prof. G. Strazzulla, director of the Catania Astrophysical Observatory, and Dr. G. Leto, responsible for the M. G. Fracastoro observing station for their warm hospitality and allowance of telescope time for the observations. This research has been also partially supported by INAF and Italian MIUR. This research has been made use of the ADS and CDS databases, operated at the CDS, Strasbourg, France and TÜBİTAK ULAKBİM Süreli Yayınlar Kataloğu.

References

Böhm-Vitense, E. 1981, ARA&A, 19, 295
Bilir S., Ak T., Soydugan E., Soydugan F., Yaz E., Ak F., Eker Z., Demircan O. & Helvacı M. 2008, AN, 329, 835
de Jager C. & Nieuwenhuijzen H. 1987, A&A, 177, 217
Cutri R. M., et al., 2003, The IRSA 2MASS All-Sky Point Source Catalog, NASA/IPAC Infrared Science Archive. http://irsa.ipac.caltech.edu/applications/Gator/
Dinescu, D.I., Girardi, T.M. & van Altena, W.F. 1999, AJ, 117, 1792
Drilling J. S. & Landolt A. U., 2000, "Allen's Astrophysical Quantities", Fouth Edition, ed. A.N.Cox (Springer), p.381
Eggleton, P. P. 1971, MNRAS, 151, 351
Ekström, S., Meynet, G., Maeder, A. & Barblan, F. 2008, A&A, 478, 467
Eldridge, J. J. & Tout, C. A. 2004, MNRAS, 353, 87
Girardi L., Bertelli G., Bressan A., Chiosi C., Groenewegen M. A. T., Marigo P., Salasnich B.& Weiss A. 2002, A&A, 391, 195
Harmanec, P. 1988, Bull. Astron. Inst. Czech., 39, 329
Hernández J., Calvet N., Briceño C., Hartmann L., Berlind P. 2004, AJ, 127, 1682
Hilditch, R. W., Howarth, I. D. & Harries, T. J. 2005, MNRAS, 357, 304
Johnson D. R. H. & Soderblom D. R. 1987, AJ, 93, 864
Kazarovets E.V., Samus, N.N., Durlevich O.V., Kireeva N.N., & Pastukhova E.N. 2006, IBVS, No.5721
Leggett, S. K. 1992, APJS, 82, 351
Lejeune, T. & Schaerer, D. 2001, A&A, 366, 538
Malkov, O. Y. 2003, A&A, 402, 1055
Malkov, O. Y. 2007, MNRAS, 382, 1073
Mihalas D. & Binney J. 1981. in Galactic Astronomy, 2nd edition, Freeman, San Fransisco, p.181
Monet,D.G. 1979, PASP, 91, 95
Munari U. & Zwitter T. 1997, A&A, 318, 269

Nordström B., Mayor M., Holmberg J., Pont F., Jorgensen B.R., Olsen E.H., Udry, S. & Mowlavi N. 2004, A&A, 418, 989
Penny R. L., Seyle D., Gies D. R., Harvin J. A., Bagnuolo W. G. Jr, Thaller M. L., Fullerton A. W. & Kaper L. 2001, ApJ, 548, 889
Prša A., Zwitter T. 2005, ApJ, 628, 426P
Pojmanski G. 2002, AcA, 52, 397
Pols, O. R., Schroder, K.-P., Hurley, J. R., Tout, C. A., & Eggleton, P. P. 1998, MNRAS, 298, 525
Queloz D., Allain, S., Mermilliod, J.-C., Bouvier, J., & Mayor, M., 1998, A&A, 335, 183
Royer, F., Gerbaldi, M., Faraggiana, R., & Gomez, A. E. 2002, A&A, 381, 105
Schaller, G., Schaerer, D., Meynet, G. & Maeder, A. 1992, A&AS, 96, 269
Schlegel D. J., Finkbeiner D. P. & Davis M. 1998, ApJ, 500, 525
Southworth J., Smalley B., Maxted P. F. L., Claret A. & Etzel P. B. 2005, MNRAS, 363, 529
Tokunaga A. T. 2000, in Cox A. N., ed., Allen's Astrophysical Quantities, 4th edn. Springer-Verlag, Berlin , p. 143
Williams, S.J. 2009, AJ, 137, 3222
van Leeuwen F. 2007, A&A, 474, 653
van Hamme, W. 1993 AJ, 106, 2096
von Zeipel, H. 1924, MNRAS, 84, 665